JOURNAL OF SOLID STATE CHEMISTRY 31, 295–303 (1980)

Electrical Conduction Studies in Ferric-Doped $KHSO_4$ Single Crystals

M. SHARON AND A. K. KALIA

Department of Chemistry, Indian Institute of Technology, Bombay, India

Received September 29, 1978; in revised form January 15, 1979

Direct-current conductivity of ferric-doped (138, 267, and 490 ppm) single crystals of $KHSO_4$ has been studied. The mechanism for the dc conduction process is discussed. It is observed that the ferric ion forms a (Fe^{3+}–two vacancies) complex and the enthalpy for its formation is 0.09 ± 0.01 eV. It is proposed that each ferric ion removes two protons from each HSO_4 dimer. The conductivity plot shows the presence of intrinsic and extrinsic regions. It is proposed that in the intrinsic region the dimer of HSO_4^- breaks reversibly to form a long-chain monomer-type structure. The conductivity in the $KHSO_4$ crystal is proposed to be controlled by the rotation of HSO_4^- tetrahedra along the axis which contains no hydrogen atom. Isotherm calculation for the trivalent-doped system is applied to this crystal and the results are compared with Co^{2+}-doped $KHSO_4$ crystal. The distribution coefficient of ferric ion in the $KHSO_4$ single crystal is calculated to be 4.5×10^{-1}. Ferric ion causes tapering in the crystal growth habit of $KHSO_4$ and it is believed to be due to the presence of (Fe^{3+}–two vacancies) complex. The enthalpy values for the various other processes are as follows: enthalpy for the breakage of HSO_4^- dimer (H_i) = 1.28 ± 0.01 eV; enthalpy for the rotation of HSO_4^- tetrahedron (H_m) = 0.58 ± 0.01 eV.

1. Introduction

There are large numbers of publications on the acid phosphates and arsenic crystals (*1–5*), but relatively fewer papers have been published on the acid sulfates, e.g., $KHSO_4$, NH_4HSO_4, $RbHSO_4$, etc. (*6, 7*). Sharon and Kalia (*7*) have studied electrical conduction and tritium diffusion with pure and doped cobalt(II) single crystals of $KHSO_4$. They have explained the results of the conductivity data by the synchronous rotation mechanism as proposed earlier by the same authors for the acid phosphate systems (*5*). It is argued that the HSO_4^- tetrahedron rotates along its axis to facilitate the migration of protons from one HSO_4 group to the other HSO_4 group. However, due to the presence of two types of HSO_4^- tetrahedra (*8*) resulting from hydrogen bond linkage (S_1 and S_2), the proton conduction mechanism in $KHSO_4$ crystals becomes a little complicated. One needs to know whether both S_1 and S_2 tetrahedra contribute toward protonic conduction or only one of them does. Because the S_1 tetrahedra exists in pairs and are linked by a double hydrogen bridge on both sides of the symmetry center, forming a double molecule, whereas the S_2 tetrahedra are linked by a bridge repeating through the glide plan (100) thus forming an infinite chain along the *a*-axis (*8–10*). In the previous paper (*7*), it was proposed that in the intrinsic region the S_1 dimer breaks up into the S_2-type structure. But the migration of protons occurs only through a synchronized rotation of the S_2-type HSO_4^- dimer (*5*). This argument was based on the electrical conduction results obtained with cobaltous(II)-doped $KHSO_4$ single crystal, where it was expected that each cobalt(II) ion would create one proton vacancy, which in turn, would facilitate the

0022-4596/80/030295-09$02.00/0

formation of the S_2-type structure from the S_1-type dimer. If this argument is extended to a crystal doped with trivalent cations (e.g., Fe^{3+} ion) then each ferric ion can create two proton vacancies in the $KHSO_4$ crystal. The question arises, which proton would be removed? There are two possible ways by which the proton vacancies can be created in the S_1 dimer, the first being the removal of both protons (i.e., two) from one single S_1 dimer and the second being the removal of two protons from two different S_1 dimers, i.e., one proton from each S_1 dimer. If the former process occurs then there is a discontinuity in the migration of protons, because the S_1 dimer has no proton to help the proton migration by the synchronous rotation process. If this happens, then the conductivity values for the ferric-doped $KHSO_4$ single crystal (i.e., for the trivalent-doped crystal) should be lower than that obtained with the cobaltous-doped $KHSO_4$ (i.e., for the divalent-doped crystal), provided both crystals contain the same concentration of dopant. However, if the latter process predominates then the conductivity in the extrinsic region should be higher for the ferric-doped crystal, because the number of S_2-type chains would have increased, which would facilitate proton migration. On the other hand, if protons are removed from the S_2 long chain, then the continuity of the chain will be disrupted, which would decrease the conductivity of the ferric-doped crystal to a large extent compared to that of the cobaltous-doped $KHSO_4$ crystal. However, one cannot rule out various other permutations and combinations and it is then to be too difficult to obtain any definite answer, unless some other physical rigorous tests are performed to locate the densities of proton vacancies in the crystals doped with the trivalent ion.

The present paper is thus an attempt to study the effect of ferric ion doping on the conductivity of the single crystal of $KHSO_4$. Attempts are made to calculate the enthalpy values for the various conduction processes by using an isotherm calculation.

2. Experimental Technique and Results

2.1. Growth of the Ferric-Doped $KHSO_4$ Single Crystal

$KHSO_4$ crystals doped with Fe^{3+} were grown by the slow evaporation technique mentioned in our previous paper (*7*). $Fe_2(SO_4)_3$ was used as the dopant salt and $^{55}Fe_2(SO_4)_3$ in H_2SO_4 (pH = 1.0) as a tracer. $^{55}Fe_2(SO_4)_3$ was prepared from $^{55}FeCl_3$ solution (obtained from BARC, India) by passing it through an anion exchange resin (IRA-420) column loaded with SO_4^{-2} ions. The eluent thus contained carrier-free $^{55}Fe_2(SO_4)_3$. The best growth rate of the crystal was observed at 25°C. The distribution coefficient of Fe^{3+} into the $KHSO_4$ crystal was calculated by the method discussed earlier (*5*). The concentration of the dopant in each crystal was obtained without destroying the crystal (*5*).

The distribution coefficient of Fe^{3+} in $KHSO_4$ single crystals was found to be 4.5×10^{-1}.

It was observed that the crystal containing ferric ions greater than 400 ppm had changed its growth habit (i.e., showed a tapering). In the presence of ferric ions the growth rate of the crystal was also found to increase by four- to five-fold. The tapering of the crystal became very obvious with ferric ion concentrations greater than 600 ppm. The effect of the tapering is shown in Fig. 1. The first three crystals from the left have ferric ion concentrations in decreasing order (i.e., 1000, 490, and 23 ppm); the fourth is pure $KHSO_4$ single crystal. The first crystal from the left is yellow in color whereas the others are colorless. This tapering effect has also been observed with KH_2PO_4 (*12*) doped with ferric ions. However, no such tapering was observed with cobalt(II) doping in $KHSO_4$ single crystal (*7*).

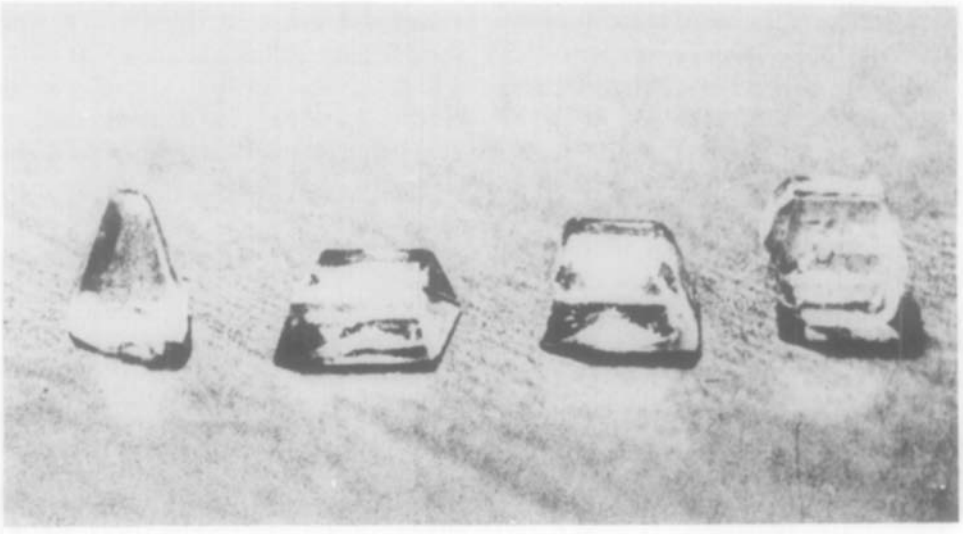

FIG. 1. Crystal of $KHSO_4$ showing the tapering due to the Fe^{3+} dopant. Crystals from left to right contain 1000, 490, and 23 ppm of Fe^{3+}; the last one is pure $KHSO_4$.

2.2. *dc Conductance Studies*

A guard ring technique (*5*) was used to measure the dc conductivity of the $KHSO_4$ single crystals. Since aluminum was found to react with the $KHSO_4$ crystal, a thin film of graphite paint was deposited on the surface of the crystal to ensure good contact. A potential of 2.0 V was applied across the central electrode only when the required temperature had been maintained by this cell for 5–10 min. The resistance was measured within 1–2 min of application of the dc potential, after which the potential was switched off. This method ensures a minimum dc electrolysis of the crystal. The conductivity was measured in the temperature range 180 to −80°C. The results were reproducible for several heating and cooling cycles. No measurements were made with pure single crystal of $KHSO_4$, as it was not necessary for the present work, because a plot of $\log \sigma T$ vs $1/T$ showed the presence of extrinsic and intrinsic regions, and extrapolation of the intrinsic region toward low temperature would give the correct conductivity values for an ideally pure single crystal of $KHSO_4$ (Fig. 2) in the extrinsic region. All conductivity measurements were made under vacuum (10^{-3} Torr).

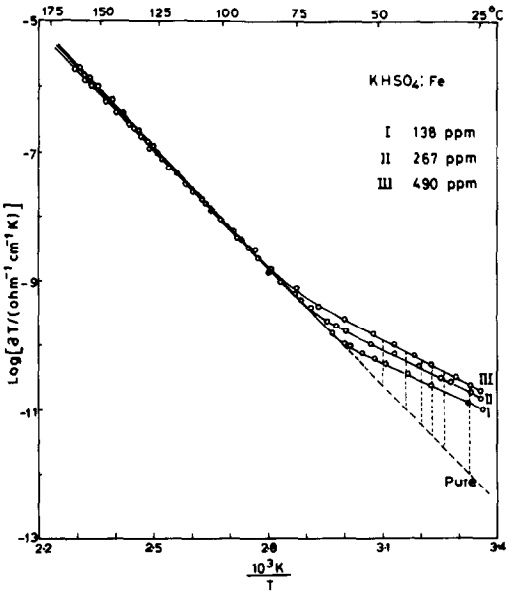

FIG. 2. Variation of conductivity values vs reciprocal of absolute temperature (T) with $KHSO_4$ doped with Fe^{3+} ions.

The dc conductance measurements of the $KHSO_4$ crystal doped with Fe^{3+} cations (138, 267, and 490 ppm) were made along the axis parallel to the c-axis. A plot of $\log \sigma T$ vs $1/T$ was then made for these crystals (Fig. 2). These plots are of the same nature as those observed with cobalt(II)-doped $KHSO_4$ (*7*). The intercepts and the slopes of the two regions (i.e., extrinsic and intrinsic) for each doped crystal were calculated by the method of least squares and, from these slopes, the enthalpies for conduction in the extrinsic and intrinsic regions were calculated (Table I). The enthalpy for the conduction (intrinsic region) is of the order of 1.22 to 1.30 eV and is comparable with the value 1.20 eV obtained with cobalt(II)-doped $KHSO_4$ crystal (*7*). However, the enthalpy for conduction in the extrinsic region, i.e., 0.56 to 0.64 eV, is higher than the value 0.48 eV obtained with cobalt(II)-doped $KHSO_4$ crystals (*7*). A typical conductivity equation for the ferric-doped $KHSO_4$ (490 ppm) single crystal is given by

$$\sigma T = 1.66\times10^{9}\exp\left(-\frac{1.28\pm0.01\ \text{eV}}{kT}\right)$$

$$+1.25\times10^{-2},\ \exp\left(-\frac{0.64\pm0.01\ \text{eV}}{kT}\right).$$

Similarly the entropy values for the extrinsic and the intrinsic regions were calculated from their respective intercepts. These values are given in Table I. The specific conductivity values (i.e., σT) at 303 and 400 K of the $KHSO_4$ crystal containing cobalt(II) and Fe^{3+} ion dopants (each crystal containing approximately the same concentration of dopant) are given below.

$KHSO_4$	$303\sigma T$ K ($\text{ohm}^{-1}\,\text{cm}^{-1}$ K)	$400\sigma T$ K ($\text{ohm}^{-1}\,\text{cm}^{-1}$ K)
(i) Cobalt doped (*7*)	2.0×10^{-10}	3.0×10^{-7}
(ii) Ferric doped	3.0×10^{-11}	1.0×10^{-7}

These values show that the conductivity values (extrinsic regions) of the crystal doped with Fe^{3+} ions are considerably lower than those for the crystal doped with cobalt(II) ions. In the intrinsic region there is little effect of these dopants. This is what one would expect to obtain. This also suggests that ferric ion must be affecting the S_1 dimer and creating two proton vacancies in the dimer.

The enthalpy for the rotation (H_R) of the HSO_4^- ions (equivalent to the mechanism proposed for KH_2PO_4 or $NH_4H_2PO_4$ (*5*)) can be calculated from the enthalpy for conduction in the intrinsic region (i.e., $H_{\text{intrinsic}} = \frac{1}{2}H_m + H_R$) provided the enthalpy for the migration of the proton (H_m) is calculated from the enthalpy for conduction in the extrinsic region ($H_{\text{extrinsic}} = H_m + \frac{1}{2}H_a 2$).

TABLE I

ENTHALPIES (H), INTERCEPTS (A), AND ENTROPY CHANGE (ΔS) FOR THE CONDUCTIVITY (ALONG THE $\perp c$-AXIS) OF THE Fe^{3+}-DOPED $KHSO_4$ SINGLE CRYSTALS[a]

Amount of dopants (ppm)	Enthalpy for conductance, $H_{\text{extrinsic}}$ (eV)	$A_{1,\text{extrinsic}}$ ($\text{ohm}^{-1}\,\text{cm}^{-1}$)	$\Delta S_{\text{extrinsic}}$ (eV K^{-1})	Enthalpy for conductance $H_{\text{intrinsic}}$ (eV)	$A_{2,\text{intrinsic}}$ ($\text{ohm}^{-1}\,\text{cm}^{-1}$)	$\Delta S_{\text{intrinsic}}$ (eV K^{-1})
138	0.56 ± 0.01	4.24×10^{-2}	-1.2×10^{-3}	1.22 ± 0.01	9.8×10^{7}	5.4×10^{-4}
267	0.56 ± 0.01	5.43×10^{-2}	-1.2×10^{-3}	1.30 ± 0.01	1.9×10^{10}	9.8×10^{-4}
490	0.64 ± 0.01	1.25×10^{-2}	-9.4×10^{-4}	1.28 ± 0.01	1.7×10^{9}	7.7×10^{-4}

[a] $\sigma T = [A_1\exp(-H/KT)]_{\text{extrinsic}} + [A_2\exp(-H/KT)]_{\text{intrinsic}}$.

However, in order to calculate the accurate values of H_m, the enthalpy for the association (H_a) of impurity–vacancy complexes must be calculated (*13*), which may be obtained from the following isotherm calculations.

2.3. Isotherm Calculations

Isotherm calculation is based on the assumption that each dopant impurity would form an impurity–vacancy complex (*17*). In the present work, the crystal is doped with iron which can exist as either Fe^{2+} or Fe^{3+} ions. If ferrous ion is present in the crystal then calculation similar to that for Co^{2+} ion (*7*) can be performed (using Eq. (2)). In this case one would assume the formation of (Fe^{2+}–vacancy) complex. On the other hand if Fe^{3+} ion is present in the crystal then it can form an (Fe^{3+}–two vacancies) complex, and then the trivalent isotherm equation (3) should be used to calculate the various enthalpy values.

Sharon and Kalia (*11*) have derived a general isotherm equation which is given as:

$$\frac{C}{\sigma/\sigma_0} = \frac{1}{n-1} x_0(1+\theta) + \frac{K_n(T)}{(n-1)^n} x_0^n (1+\theta)^{n-1} \left(\frac{\sigma}{\sigma_0}\right)^{n-1}. \quad (1)$$

One obtains, for a divalent-doped system (i.e., $n = 2$),

$$\frac{C}{\sigma/\sigma_0} = x_0(1+\theta) + K_2(T) x_0^2 (1+\theta)^2 \left(\frac{\sigma}{\sigma_0}\right), \quad (2)$$

which is similar to the equation derived by Lidiard (*17*); For the trivalent-doped system (i.e., $n = 3$) one obtains

$$\frac{C}{\sigma/\sigma_0} = \frac{x_0(1+\theta)}{2} + \frac{K_3(T)}{8} x_0^3 (1+\theta)^3 \left(\frac{\sigma}{\sigma_0}\right)^2, \quad (3)$$

where

C = concentration of dopant

σ_0 = specific conductivity of a pure crystal at temperature T (in the extrinsic region)

σ = specific conductivity of the single crystal doped with an impurity of C concentration at temperature T (in the extrinsic region)

$x_0 = x_1 x_2$, where x_1 and x_2 are the molar fractions of two complimentary intrinsic defects

$K_n(T)$ = equilibrium constant for the quasi-chemical reaction: Unassociated $(+n)$–valent impurity ions + unassociated vacancies $\rightleftharpoons$ (impurity $(n-1)$–vacancy complex)

$\theta = u_2/u_1$, where u_2 and u_1 are the mobilities of the two complementary defects (i.e., x_1 and x_2); however, with these crystals $u_2 = 0$(6), and hence $\theta = 0$

n = valence state of the dopant

Both Eqs. (2) and (3) would give a linear plot and from the slopes and the intercepts of the two plots the enthalpy values for the various conduction processes can be calculated. But only one of the two equations would show a correct enthalpy value for the ferric-doped $KHSO_4$ single crystal.

2.31. Isotherm Calculations from Eq. (2) (i.e., where $n = 2$). A plot of $C/(\sigma/\sigma_0)$ vs (σ/σ_0) was made (Fig. 3). The slope and the intercept of each isotherm were calculated by the method of least squares. From these values the molar concentration of x_0 and the equilibrium constant $K_2(T)$ for the different temperatures were calculated. Since both these terms (i.e., x_0 and $K_2(T)$) have an activation energy (*5*), plots were made of $\log x_0$ vs $1/T$ (Fig. 4) and $\log K_2$ vs $1/T$ (Fig. 5) to calculate the enthalpy values. From the slopes of these linear plots, the enthalpy for the formation of intrinsic defect ($H_{R_{Fe}2+}$) and the enthalpy for the association of (Fe^{2+}–vacancy) complex ($H_{a_{Fe}2+}$) were calculated respectively. These values are shown in Table II. The enthalpy for migration of the defects was calculated from the equation

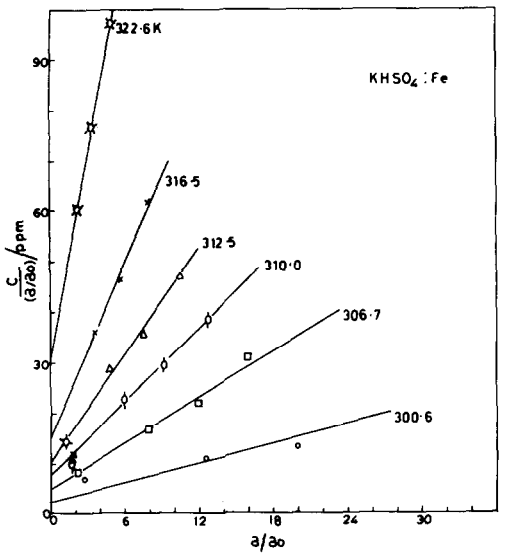

FIG. 3. Variation of $C/(\sigma/\sigma_0)$ vs σ/σ_0 for $n = 2$.

$H_{\text{extrinsic}} = \frac{1}{2}H_{a_{Fe}2+} + H_m$, where $H_{\text{extrinsic}}$ is the experimentally observed value (from Fig. 2) and $H_{a_{Fe}2+}$ is calculated from isotherm calculation. Once H_m is calculated enthalpy for the formation of defect ($H'_{R_{Fe}2+}$) can also be calculated from the equation $H_{\text{intrinsic}} = \frac{1}{2}H'_{R_{Fe}2+} + H_{m_{Fe}2+}$ (*13*) where $H_{\text{intrinsic}}$ is the experimentally observed value (from Fig. 2) and $H_{m_{Fe}2+}$ is calculated from $Ha_{Fe}2+$. All these values are shown in Table II. This calculation was made to confirm whether iron has occupied as Fe^{2+} state in the crystal.

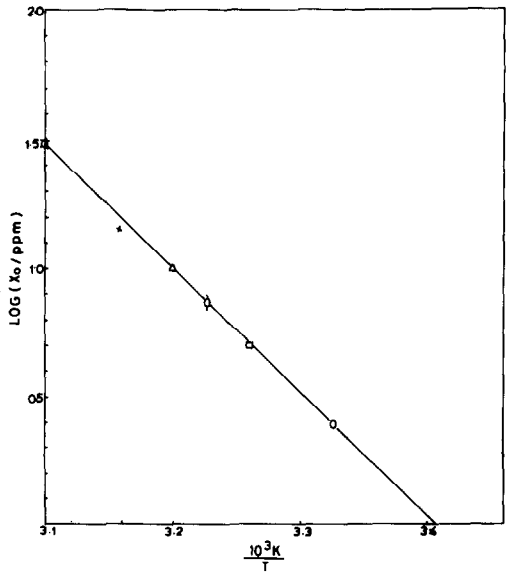

FIG. 4. Variation of $\log x_0$ vs $1/T$ for $n = 2$ (Fe^{3+}-doped $KHSO_4$).

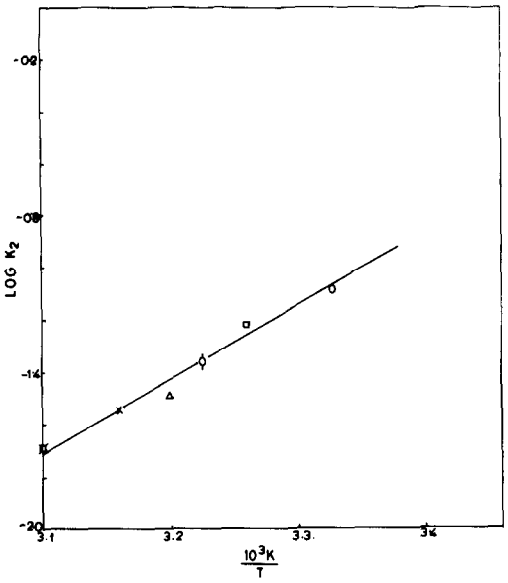

FIG. 5. Variation of $\log K_2$ vs $1/T$ for $n = 2$ (Fe^{3+}-doped $KHSO_4$).

TABLE II

ENTHALPY VALUES CALCULATED FOR THE $KHSO_4$ CRYSTAL DOPED WITH Fe^{3+} IONS AND Co^{2+} IONS

	eV		eV
$H_{R_{Co}2+}$ [a]	1.18±0.01	$H_{a_{Fe}2+}$	0.56±0.01
$H_{m_{Co}2+}$ [b]	0.55±0.01	$H'_{R_{Fe}2+}$ [c]	2.04±0.01
$H_{a_{Co}2+}$ [d]	−0.14±0.01	$H_{R_{Fe}2+}$	1.28±0.01
$H'_{R_{Co}2+}$	1.30±0.01	$H_{m_{Fe}3+}$	0.58±0.01
$H_{R_{Fe}2+}$	1.87±0.01	$H_{a_{Fe}3+}$	0.09±0.01
$H_{m_{Fe}2+}$	0.25±0.01	$H'_{R_{Fe}3+}$	1.38±0.01

[a] All H_R values are calculated from the equation $x_0 = \exp(-H_R/kT)$.

[b] All H_m values are calculated from the equation $H_{\text{extrinsic}} = (1/n)H_a + H_m$.

[c] All H'_R values are calculated from the equation $H_{\text{intrinsic}} = \frac{1}{2}H'_R + H_m$.

[d] All H_a values are calculated from the equation $K_n(T) = Z\exp(-H_a/kT)$.

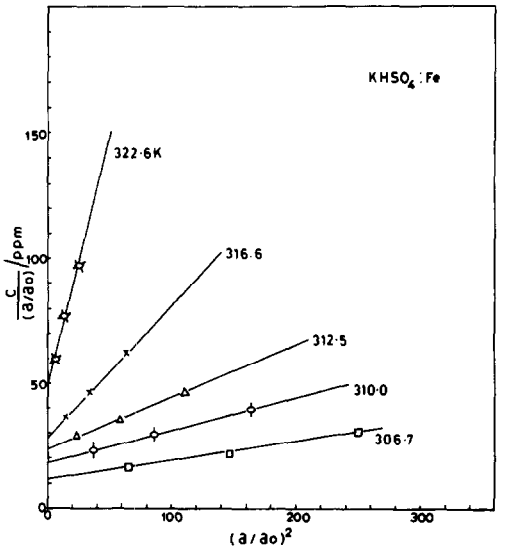

FIG. 6. Variation of $C/(\sigma/\sigma_0)$ vs $(\sigma/\sigma_0)^2$ for $n = 3$.

If it has, then one would expect $H_{a_{Co}2+} \approx H_{a_{Fe}2+}$ and $H_{R_{Co}2+} \approx H'_{R_{Co}2+} \approx H'_{R_{Fe}2+}$. From Table II it is clear that this is not the case. Hence, further calculations were made with Eq. (3).

2.32. Isotherm Calculations from Eq. (3) (i.e., where $n = 3$). Similar calculations were repeated using Eq. (3). However, in this case a plot of $C/(\sigma/\sigma_0)$ vs $(\sigma/\sigma_0)^2$ was made (Fig. 6). In similar fashion x_0 (Fig. 7) and $K_3(T)$ (Fig. 8) were calculated for different temperatures, and from these $H_{R_{Fe}3+}$ and $H_{a_{Fe}3+}$ were calculated. The calculation of $H_{m_{Fe}3+}$ was made by using the general equation derived by Sharon and Kalia (7) with $n = 3$, i.e., $H_{\text{extrinsic}} = H_{m_{Fe}3+} + 1/3H_{a_{Fe}+3}$. Similarly $H'_{R_{Fe}3+}$ was calculated by using the equation $H_{\text{intrinsic}} = H'_{R_{Fe}3+} + 1/2H_{m_{Fe}3+}$. The enthalpy values obtained by these calculations are shown in Table II.

The comparison of $H_{R_{Co_2}}$, $H_{m_{Co_2}}$, $H_{R_{Fe}3+}$, and $H_{m_{Fe}3+}$ values show that they are comparable (Table II). This suggests that iron-doped $KHSO_4$ contains mainly ferric ions and not ferrous ions.

3.1. Mechanism for Conduction

The isotherm calculations have confirmed that the iron-doped $KHSO_4$ single crystal contains mainly ferric ions and not ferrous ions.

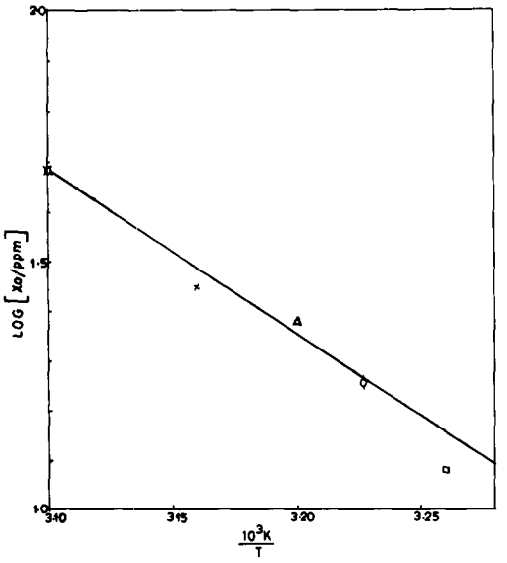

FIG. 7. Variation of $\log x_0$ vs $1/T$ for $n = 3$ (Fe^{3+}-doped $KHSO_4$).

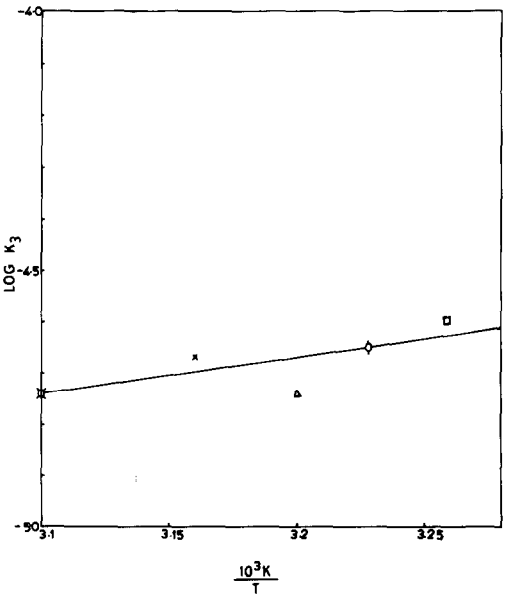

FIG. 8. Variation of $\log K_3$ vs $1/T$ for $n = 3$ (Fe^{3+}-doped $KHSO_4$).

The next pertinent question to understand is the mechanism of the conduction in $KHSO_4$ and then to assign these enthalpy values for the corresponding processes.

$KHSO_4$ contains two types of distinct HSO_4^- tetrahedra in the crystal. One is a long chain (S_2 type) similar to the phosphate structure, forming an infinite chain along the a-axis. The other is a dimer structure (S_1 type) in which the tetrahedra are linked by double hydrogen bridges on both sides of the symmetry center, forming a double molecule. Each dimer is an entity of its own and is not connected with another dimer (*8*, *14–16*). If the conduction is to take place via the monomer chain-type structure (S_2 type) and if the synchronous rotation mechanism is operative (*5*) then one would not expect a break in the conductivity plot. On the other hand, if conduction occurs through the S_1-type dimer, then it will show a two-step process (Fig. 9). First, the dimer will have to break to form the S_2-type structure. Then the proton migration would occur through rotation of the newly formed S_2-type structure. The breakage of the dimer requires high temperatures. In other words, at high temperature more of the S_1-type dimers would break into the S_2-type chain thus increasing the population of the S_2-type chain. This increase of the long-chain S_2-type would correspondingly increase the conductivity values of the crystal. There would be a critical temperature, however, below which the breakage of the S_1-type dimer would not occur.

Therefore, conduction of crystals at low temperature will be due to the S_2-type structure, while at high temperature it will be due to the S_2-type structure initially present plus that due to newly formed S_2-type structure from the S_1-type dimer. These two processes would show a break in the conductivity plot. This is what we have observed. The enthalpy of conduction ($H_{R_{Fe^{3+}}}$ or $H'_{R_{Fe^{3+}}}$) at high temperature would be equivalent to the enthalpy for the breakage of the S_1-type dimer to the S_2-type long chain (Hi), whereas, at lower temperature the enthalpy for conduction would be due to enthalpy for the rotation of the HSO_4 tetrahedron (H_m). The mechanism by which the S_1-type structure becomes S_2 type is shown in Fig. 10 (steps 1–2). The proton from the end of the structure is discharged at the cathode (step 3). After this, rotation of HSO_4 tetrahedron occurs through the axis containing no covalent bonded hydrogen (step 4). In doing so, after every proton removal, one HSO_4 group is converted into an SO_4 group

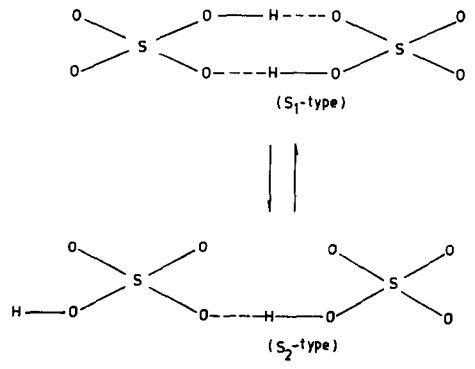

FIG. 9. Transition between the S_1- and the S_2-type structure at high temperature.

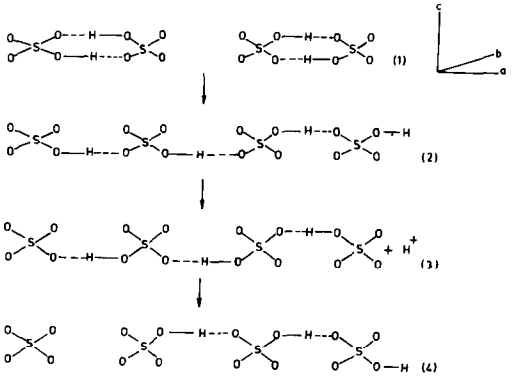

FIG. 10. Synchronous rotation conduction mechanism in single crystals of $KHSO_4$.

(step 4), which would suggest that after a prolonged dc electrolysis the $KHSO_4$ crystal would become the K_2SO_4 type.

State (III) is very similar to the S_2-type structure whereas state (IV) is much different from either the S_1- or the S_2-type tetrahedron and has no proton to help in the migration by the rotation process. It is worth mentioning that though the $KHSO_4$ crystals show conductivity plots similar to NaCl-type conductivity plots, the mechanism of the proton migration in $KHSO_4$ is entirely different from the mechanism of vacancy migration process in NaCl crystals.

Acknowledgments

One of us (A.K.K.) is thankful to the UGC for providing a Junior Research Fellowship to carry out this experiment. We are thankful to Professor H. J. Arnikar for his help in continuing this work in the Chemistry Department of Pune University.

References

1. J. M. POLLOCK AND M. SHARAN, *J. Chem. Phys.* **47**, 4067 (1967).
2. J. M. POLLOCK AND M. SHARAN, *J. Chem. Phys.* **41**, 3604 (1969).
3. L. B. HARRIS AND G. J. VELLA, *J. Chem. Phys.* **58**, 4550 (1973).
4. L. GLASSER, *Chem. Rev.* **75**, 21 (1975).
5. M. SHARON AND A. K. KALIA, *J. Solid State Chem.* **21**, 171 (1977).
6. M. SHARON AND A. K. KALIA, *J. Chem. Phys.* **66**, 3051 (1977).
7. M. SHARON AND A. K. KALIA, *J. Solid State Chem.* **20**, 53 (1977).
8. L. H. LOOPSTRA AND C. H. MACGILLAVRY, *Acta Crystallogr.* **11**, 349 (1958).
9. S. ODA, *J. Chem. Soc. Japan*, **60**, 163 (1939).
10. D. W. J. CRUICKSHANK, *Acta Crystallogr.* **11**, 349 (1958).
11. M. SHARON AND A. K. KALIA, *Indian J. Chem.* **15A**, 549 (1977).
12. J. J. GILMAN, "The Art and Science of Growing Crystals," p. 197, Wiley, New York (1963).
13. P. W. DREYFUS AND A. S. NOWICK, *Phys. Rev.* **126**, 1367 (1962).
14. P. GROTH, "Element der Physikalischen and Chemischem Krystallographie," p. 174, Oldenbourg Verlag, Munich (1921).
15. S. Oda, *J. Chem. Soc. Japan* **60**, 163 (1959).
16. D. W. J. CRUICKSHANK, *Acta Crystallogr.* **11**, 349 (1958).
17. A. B. Lidiard, "Handbook Der Physik," Vol. 20, p. 246, Springer-Verlag, Berlin/New York (1957).